



## **Electroless deposition of nickel microbumps for fine-pitch flip-chip bonding**

Downloaded from: <https://research.chalmers.se>, 2024-07-27 10:56 UTC

Citation for the original published paper (version of record):

Lu, Y., Lin, C., Wang, S. et al (2024). Electroless deposition of nickel microbumps for fine-pitch flip-chip bonding. *Journal of Physics: Conference Series*, 2783(1).  
<http://dx.doi.org/10.1088/1742-6596/2783/1/012022>

N.B. When citing this work, cite the original published paper.

# Electroless deposition of nickel microbumps for fine-pitch flip-chip bonding

Yu Lu <sup>1</sup>, Chang Lin <sup>1,2,5</sup>, Shuaishuai Wang <sup>1</sup>, Kaixin Zhang <sup>1,6</sup>, Taifu Lang <sup>1</sup>, Yang Li <sup>1</sup>, Qiwei Li <sup>1</sup>, Tianxi Yang <sup>2</sup>, Zhonghang Huang <sup>2</sup>, Chunli Yan <sup>4</sup>, Jie Sun <sup>1,2,3</sup>, and Qun Yan <sup>1,2</sup>

<sup>1</sup>National and Local United Engineering Laboratory of Flat Panel Display Technology, College of Physics and Information Engineering, Fuzhou University, Fuzhou, 350100, China

<sup>2</sup>Fujian Science & Technology Innovation Laboratory for Optoelectronic Information of China, Fuzhou, 350100, China

<sup>3</sup>Quantum Device Physics Laboratory, Department of Microtechnology and Nanoscience, Chalmers University of Technology, Gothenburg, 41296, Sweden

<sup>4</sup>Department of Information and Automation, Fuzhou University, Fuzhou, 350108, China

<sup>5</sup>Corresponding author's e-mail: linchang@fjoel.cn

<sup>6</sup>Corresponding author's e-mail: 316964@fzu.edu.cn

**Abstract:** The reliability of micro-light-emitting diode (Micro-LED) is closely associated with the uniformity of microbumps arrays. With continual decreases in pixel pitch in recent years, it is a challenge to guarantee the uniformity of bump arrays. To satisfy current requirements for ultra-high-density interconnections, this study proposes an electroless plating method for fabricating highly uniform nickel microbumps. This technique differs from electroplating, in which the morphology and consistency of microbumps can be easily controlled. Furthermore, it is a high-selectivity and cost-effective method of microbumps fabrication that eliminates solder wastage and avoids metal lift-off in traditional evaporation. To minimize the non-uniformity of the bumps, we aim to optimize the oxygen plasma treatment parameters and deposition intervals to eliminate the issues of skip plating, hydrogen bubble entrapment, and nodules. Under the combined effect of plasma treatment and intermittent deposition method, microbump arrays with less than 5% non-uniformity were successfully prepared, achieving the demands of high-density bonding. In addition, the preparation process is highly reproducible, extending the application range of this technique.

## 1. Introduction

Micro-LED has unsurpassed advantages in terms of lifetime, brightness, response speed, and power consumption, so it can engage the interest of many researchers [1-2]. Notably, the pixel size of Micro-LED ranges from 1  $\mu\text{m}$  to 50  $\mu\text{m}$ , allowing for high-density integration on a single chip and resulting in a display device with an ultra-high resolution that can satisfy the demand for high-quality visual effects. In the Micro-LED manufacturing process, flip-chip bonding is a critical technology that determines the Micro-LED's reliable performance and display effect. However, as the display pixel pitch has shrunk over the past few years, the ultra-high-density interconnection will make bonding more challenging.



High-uniformity bump arrays are essential for bonding yields and display device quality, and current procedures for preparing Micro-LED bumps include electroplating [3], evaporation [4], and electroless plating [5]. Electroplating is an electrochemical process that requires the introduction of current during the preparation process. The uniformity of the current distribution will immediately impact the coplanarity and morphology of the bump array. Due to the sensitivity of the current distribution to parameters such as ion concentration distribution in the plating solution, the distance between electrodes, parallelism, and shape, it is not easy to guarantee the regularity and high consistency of the bumps. Evaporation is a physical deposition that necessitates expensive apparatus and high vacuum conditions, resulting in substantial financial and time consumption. As the pixel size and pitch continue to shrink, metal mask lift-off-related issues tend to arise and make the high consistency of the microbump more challenging. Electroless plating is a highly selective deposition and cost-effective technology, and the process procedures and equipment involved are relatively simple. Our previous research proposed using electroless plating to prepare nickel microbumps to interconnect ultra-high-density Micro-LED with a driving circuit board. The prepared bumps have a regular morphology, and there are no impurities and voids inside the bumps, which confirms that it is a feasible and practical approach [6]. Unfortunately, previous studies have not investigated the uniformity of bump arrays, and the existing studies on bump consistency have concentrated on large-feature-sizes and low-density bump arrays [3, 4, 7], leaving much space for exploration of small-dimension bump arrays with pitch inside 10  $\mu\text{m}$ . Besides, there are several urgent concerns during the fabrication process, such as skip plating, hydrogen bubble entrapment, and nodular growth, which will be discussed in detail in the subsequent chapter.

In this study, we propose a method for electroless plating high-uniformity nickel pillar microbump arrays for ultra-fine-pitch chip bonding. Three types of deposition defects in the experiments are identified, and their formation causes are individually discussed and analyzed. To address the underlying causes, we introduced oxygen plasma treatment into the preparation procedure and optimized the plasma treatment time. The results indicate that the photolithographic pattern has improved plating properties and wettability after 4 minutes of plasma treatment and the surface contact angle of only  $32.9^\circ$ , which may mitigate bump defects to a greater extent. In addition, intermittent electroless nickel plating is implemented to eliminate the influence of hydrogen bubbles and reduce the non-uniformity of the bumps. It has been determined that when the periodic time is set to 4 minutes, the uniformity of the bump array is within 5%, which satisfies the requirements of ultra-high-density interconnects. The preparation process is highly repeatable, which facilitates the popularization and application of this process technology and plays a crucial role in guiding the advancement of the essential technology of Micro-LED interconnections.

## 2. Material and methods

### 2.1. Photolithography

Figure 1 displays the complete fabrication flow of the nickel microbump. Cr/Al/Ti/Pt/Au was evaporated on a 4-inch silicon wafer, followed by sputtered 100-nm-thick nickel film as a seed layer. Afterward, the wafer was diced into individual dies and rigorously cleaned with acetone and isopropanol to remove contamination. The 7- $\mu\text{m}$ -thick positive photoresist was spin-coated on the seed layer and exposed to ultraviolet light at a dose of  $1025 \text{ mJ/cm}^2$ . After development for 2 minutes, a lithographic pattern structure with a pitch of 8  $\mu\text{m}$  and a diameter dimension of 5-6  $\mu\text{m}$  was successfully obtained.

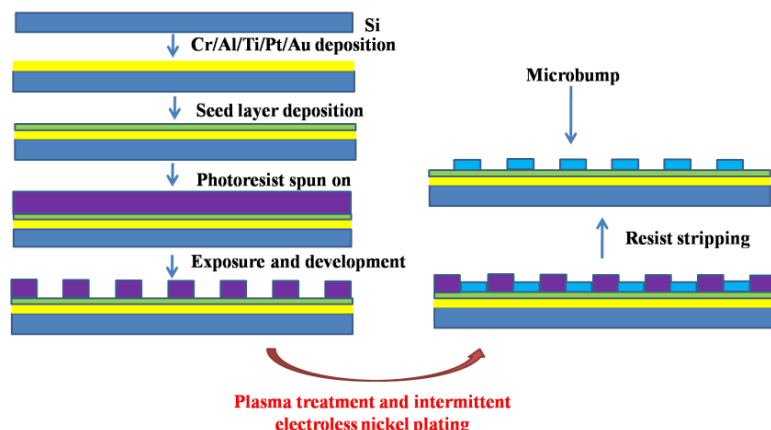


**Figure 1.** Flow chart of the electroless nickel plating process.

**2.2. Pretreatment process and electroless nickel plating**

Prior to conducting electroless nickel plating, greases and oxides were removed from the surface of the catalytic layer by degreasing for 3 minutes and activating for 5 minutes. The specimens were placed in plasma cleaner for surface modification following thorough rinsing in DI water and drying with nitrogen gas, and the treatment process parameters were listed in Table 1. The specimen was subsequently affixed to a glass and inserted vertically into the plating solution at 75°C and a pH of 5 with the stirrer speed set at 150 rpm, as depicted in Figure 2. Two plating patterns were continuous deposition and intermittent deposition, and significant parameters related to plating patterns, such as deposition interval time, stagnant time, and total plating time, will be discussed in the following chapter.

**Table 1.** Key parameters of the plasma modification.

| Plasma treatment parameter | Value     |
|----------------------------|-----------|
| Chamber pressure (mbar)    | <=100     |
| Gas flow (sccm)            | 300       |
| Plasma power (W)           | 500       |
| Treatment time (min)       | 1/2.5/4/5 |

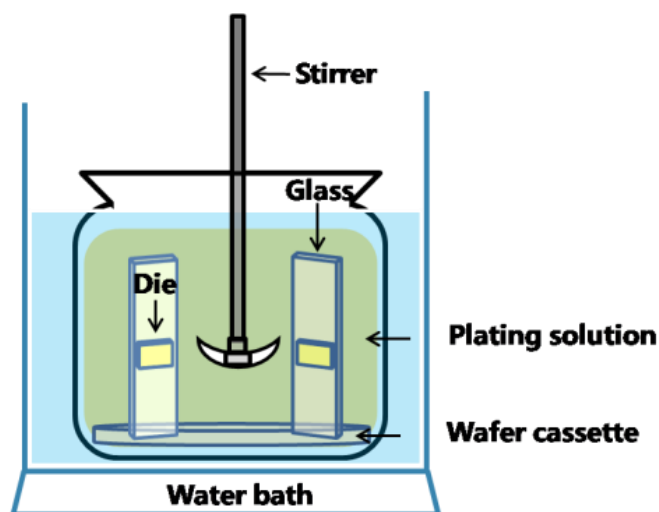


**Figure 2.** Schematic illustration of electroless deposition apparatus.

### 2.3. Characterization

Optical microscopy and three-dimensional (3D) laser microscopy were employed to observe the uniformity of the microbump. Microbump morphology was observed by using scanning electron microscopy (SEM), and cross-sectional observation was performed by using a focused ion beam (FIB). The wettability of the microstructure was analyzed by using an optical contact angle meter (SL200k).

## 3. Result and discussion

### 3.1. Defect of nickel microbumps

Electroless nickel plating is an autocatalytic redox reaction. It is noted that the reaction must occur on the surface of the substrate with catalytic activity, demanding complete contact between the plating solution and the surface of the catalytic layer. However, as shown in Figure 3 (a), a thin photoresist layer persisted at the bottom of some microporous structures due to inadequate exposure or development. The photoresist layer prevented the plating solution from contacting the substrate of the catalytic layer, inhibiting the reaction and resulting in skip plating.

Hydrogen gas is produced throughout the reaction process when nickel metal is deposited. As shown in Figure 3 (b), hydrogen bubbles are randomly attached to the surface of some patterns, which is not conducive to the reactive ions from the plating solution into and out of the microporous structure and will negatively impact the mass transfer efficiency during the reaction process. A diminishing concentration of nickel ions in the microporous structure affects the bump growth rate, resulting in different thicknesses between bubble-intensive and bubble-free regions, which severely compromise the array's coplanarity. Therefore, the accumulation of hydrogen bubbles on the surface of photolithographic patterns must be avoided.

The optical micrograph of a bump array obtained by direct plating following photolithography is illustrated in Figure 4 (a). Numerous black dots of various dimensions are arbitrarily dispersed across the array region. The black dots morphology was further analyzed by SEM, and the results are shown in Figure 4 (b)-(d). The results demonstrate that the black dots are irregular bump structures with nodular growths of diverse dimensions on the bump surface. In addition, the bump in the red circle of Figure 4 (e) was sliced with a focused ion beam, the heights of the nodules were measured, and the results are displayed in Figure 4 (f). It can be found that the height of the nodular growth is approximately one-third of the height of the bump, which will increase the difficulty of subsequent bonding and impact the bonding yield. The reason considered is that some of the impurity particles can easily attach to the bottom and patterned surface of the microstructure during the preparation process. The surface of the irregular particle shape is susceptible to nickel deposition, which serves as a nucleation site for nickel plating.

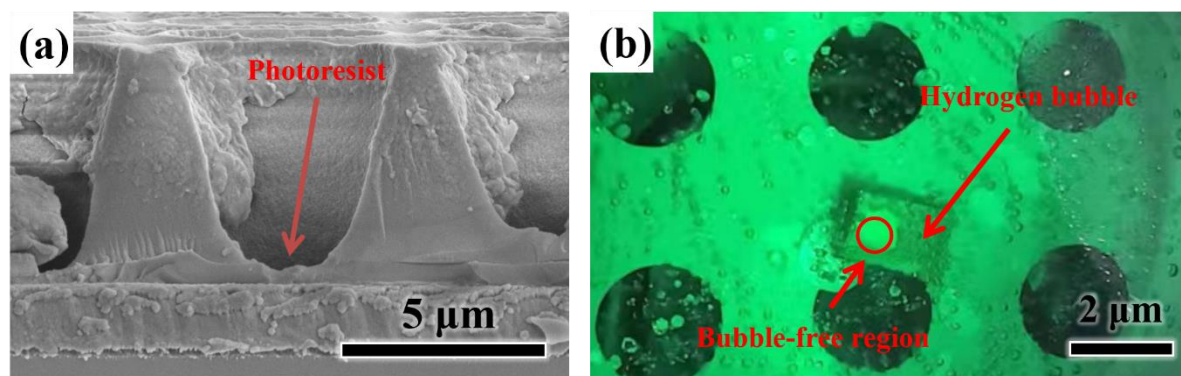


**Figure 3.** (a) SEM images of microporous structures; (b) Photograph of the specimen during electroless plating.

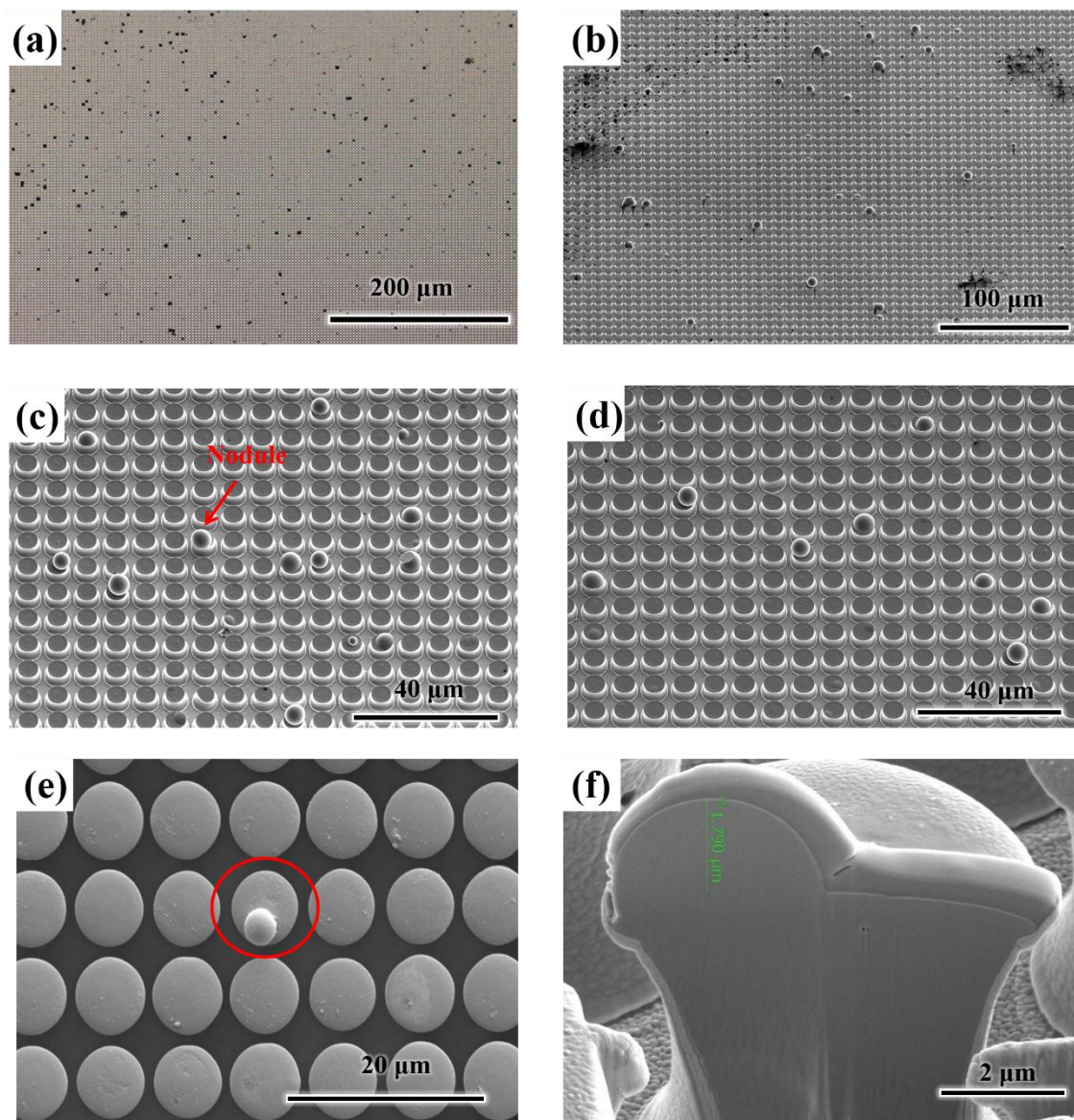


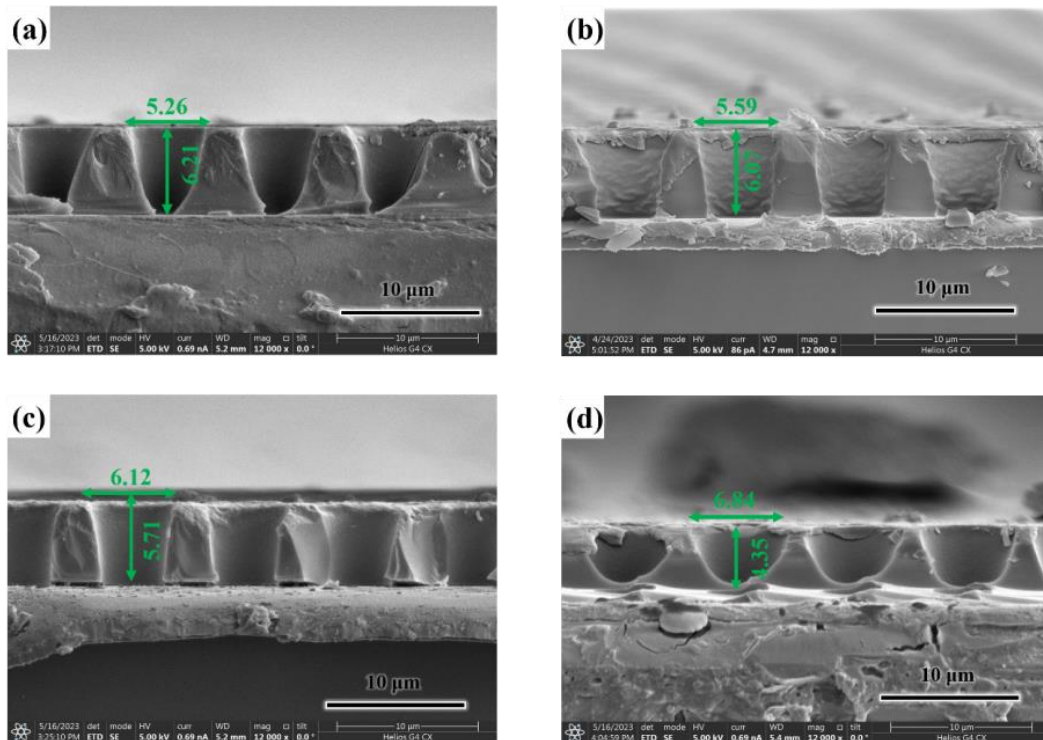
**Figure 4.** (a) Optical photographs of the bump array at 10X; (b) SEM images of the nodular morphology at 1000X; (c-d) SEM images of the array of bumps on the left and right sides of the specimen; (e) SEM images of the array of bumps in the top view; (f) Cross-section SEM image corresponding to the red circle in (e).

### 3.2. Method for the elimination of the defect of nickel microbumps

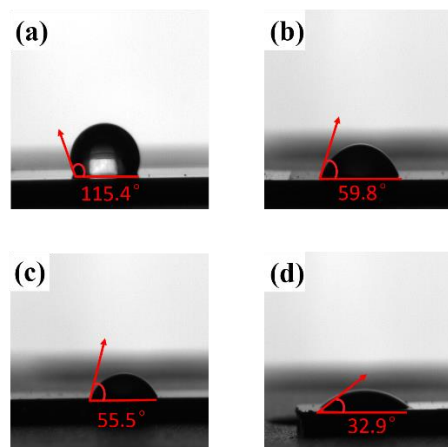
Oxygen plasma treatment is currently the frequently employed means of surface modification. Under high-frequency and high-pressure conditions, the photoresist and impurity particles remaining at the bottom of the microstructure are eliminated by the excited plasma colliding with the specimen surface. Therefore, the oxygen plasma treatment process is introduced in our research and optimizes the process parameters for the treatment time.

Figure 5 (a)-(d) provides the cross-sectional morphology of the microporous structure after the patterned surface was treated with oxygen plasma for 1, 2.5, 4, and 5 minutes, respectively. It can be seen that the seed layer is entirely exposed after 2.5 minutes of treatment because there is hardly any photoresist residual at the bottom of the photoresist pattern. The microporous structure's thickness and size changed to 4.35  $\mu\text{m}$  and 6.84  $\mu\text{m}$  after 5-minute high-energy ion collisions with the photoresist

pattern, which significantly affected the patterned structure's plating performance and rendered it unusable as a mold for electroless nickel plating. Additionally, this investigation analyzes the change of wettability by the contact angle of the plasma-treated photoresist surface, and the specific measurement results are shown in Figure 6 (a)-(d). It can be seen that the contact angle of the patterned surface decreases swiftly from  $115.4^\circ$  to  $59.8^\circ$  when the plasma modification operates for 1 minute, indicating that the patterned surface changes from hydrophobicity to hydrophilicity. Furthermore, the contact angle of the pattern's surface is only  $32.9^\circ$  after 4-minute plasma treatment, which produces superior wetting properties.



**Figure 5.** Cross-section SEM images of the photoresist pattern after oxygen plasma treatment. (a) Plasma treatment for 1 min; (b) Plasma treatment for 2.5 min; (c) Plasma treatment for 4 min; (d) Plasma treatment for 5 min.



**Figure 6.** The contact angle image of the photoresist pattern after oxygen plasma treatment. (a) Without plasma treatment; (b) Plasma treatment for 1 min; (c) Plasma treatment for 2.5 min; (d) Plasma treatment for 4 min.

The specimen was immediately handled for electroless deposition following a 4-minute oxygen plasma modification. Due to the improvement in wetting property, the number of hydrogen bubbles attached to the photoresist surface decreased substantially during the reaction procedure. Some bubbles remained and could not be removed by mechanical shaking of the specimen. In this work, intermittent electroless nickel plating was utilized to further eliminate bubbles, and the reaction process was divided into multiple cycles, as depicted in Figure 7 (a). Each cycle consists of both a reactive period and a stagnant period. In this instance, the stagnant period refers to exposing the specimen to an air environment, where the surface tension of the bubble cannot be maintained due to the pressure difference between both the interior and exterior of the bubble, causing the bubble to rupture and accomplishing the complete elimination of the bubble. Table 2 summarizes the bump array's uniformity under three distinct plating conditions. Both plasma pretreatment and intermittent plating may enhance the consistency of bump arrays. Under the combined effect of plasma pretreatment for 4 minutes and deposition interval for 4 minutes, the uniformity of the bump array reaches the optimal value of 4.64%. Besides, as shown in Figures 7 (b) and (c), the prepared microbumps have regular morphology and are devoid of voids and impurities, allowing for an excellent electrical connection.

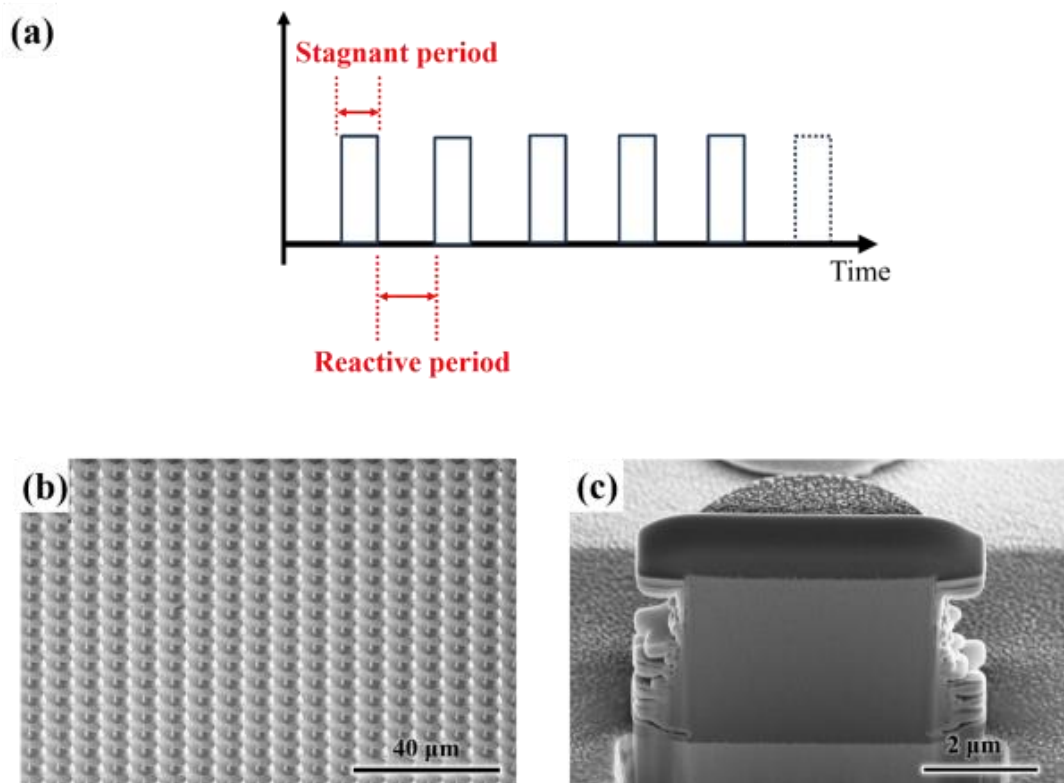


**Figure 7.** (a) Intermittent electroless nickel process in this study; (b) SEM images of microbump array with deposition interval for 4 minutes; (c) Cross-section SEM of single microbump with deposition interval for 4 minutes.

**Table 2.** Uniformity of bumps under three distinct plating conditions.

| Plasma time | Deposition interval time | Height1 | Height2 | Height3 | Height4 | Height5 | Uniformity |
|-------------|--------------------------|---------|---------|---------|---------|---------|------------|
| 4           | 0                        | 2.98    | 3.59    | 3.32    | 3.25    | 3.37    | 9.23%      |
| 4           | 5                        | 2.75    | 3.25    | 3.21    | 3.16    | 3.09    | 8.09%      |
| 4           | 4                        | 3.27    | 3.41    | 3.23    | 3.11    | 3.16    | 4.64%      |



#### 4. Conclusion

This investigation demonstrates the chemical plating method for preparing nickel microbump arrays appropriate for ultrahigh-density interconnects. We illustrate three kinds of bump defects appearing during the preparation process and optimize the oxygen plasma modification time to effectively improve the phenomena of photoresist residue, hydrogen bubble retention, and nodular growths. Furthermore, an intermittent deposition method was employed to eliminate the hydrogen bubbles on the surface of the photoresist pattern. It was discovered that when the intermittent time was set to 4 min, the inside of prepared bumps with regular morphology was void-free and dense. Most importantly, the uniformity of microbump array is stabilized to within 5%, offering a critical benchmark for Micro-LED high-density interconnection technology.

#### Acknowledgments

We thank the support from the National Key Research and Development Program of China (No. 2023YFB3608703), Fujian Science & Technology Innovation Laboratory for Optoelectronic Information of China (No. 2021ZZ122), Hunan Provincial Project (No. 2020GK2064), and Fujian Provincial Projects (No. 2021HZ0114 and No. 2021J01583).

#### References

- [1] Chen C. J., Chen H. C., Liao J. H., Yu C. J., and Wu M. C. Fabrication and Characterization of Active-Matrix 960 x 540 Blue GaN-based Micro-LED Display. *IEEE J. Quantum Electron.* 2019, 55 (2), 6, Article. <https://doi.org/10.1109/jqe.2019.2900540>.
- [2] Wang Z., Shan X. Y., Cui X. G., and Tian P. F. Characteristics and techniques of GaN-based Micro-LEDs for application in the next-generation display. *J. Semicond.* 2020, 41 (4), 6, Review. <https://doi.org/10.1088/1674-4926/41/4/041606>.
- [3] Huang J. T., Hsu H. J., Lee K. Y., Tsai T. C., and Chen C. K. High Coplanarity and Fine Pitch Copper Pillar Bumps Fabrication Method. *Jpn. J. Appl. Phys.* 2010, 49 (6), 3, Article. Proceedings Paper. <https://doi.org/10.1143/jjap.49.06gn07>.
- [4] Volpert M., Roulet L., Boronat J. F., Borel I., Pocas S., and Ribot H. Indium Deposition Processes for Ultra Fine Pitch 3D Interconnections. In 60th Electronic Components and Technology Conference, 2010, pp. 1, 739-1, 745. <https://doi.org/10.1109/ectc.2010.5490736>.
- [5] Rohan J. F., O'Riordan G., and Boardman J. Selective electroless nickel deposition on copper as a final barrier/bonding layer material for microelectronics applications. *Appl. Surf. Sci.* 2002, 185 (3-4), 289-297, Article. [https://doi.org/10.1016/s0169-4332\(01\)00982-5](https://doi.org/10.1016/s0169-4332(01)00982-5).
- [6] Tian L., Lin C., Pan K., Lu Y., Deng L., Huang Z., Yang T., Zhang Y., Sun, J., and Yan Q. Electroless Deposition of 4  $\mu\text{m}$  High Ni/Au Bumps for 8  $\mu\text{m}$  Pitch Interconnection. *ACS Electronic Materials*, 2022, 4 (10), 4, 966-4, 971. <https://doi.org/10.1021/acsaelm.2c00974>.
- [7] Du Y. X., Song Z., Zhu H. Z., and Wang Z. Y. Fabrication of Ni Microbumps with Small Feature Size on Au Using Electroless Ni Plating with Noncontact Induction. *IEEE Trans. Compon. Manuf. Technol.* 2015, 5 (8), 1, 169-1, 177, Article. <https://doi.org/10.1109/tcpmt.2015.2448683>.